Physical and Chemical Characterization of Collagen/Alginate/Poly(Vinyl Alcohol) Scaffold with the Addition of Multi-Walled Carbon Nanotube, Reduced Graphene Oxide, Titanium Dioxide, and Zinc Oxide Materials

Rusyda Fajarani[1], Siti Fauziyah Rahman[1,2*], Azizah Intan Pangesty[2,3],
Puspita Anggraini Katili[1,2], Don-Hee Park[4,5], Basari[1,2]

[1]Department of Electrical Engineering, Faculty of Engineering, Universitas Indonesia, Kampus UI Depok, West Java 16424, Indonesia
[2]Research Center for Biomedical Engineering, Faculty of Engineering, Universitas Indonesia, Kampus UI Depok, West Java 16424, Indonesia
[3]Department of Metallurgical and Materials Engineering, Faculty of Engineering, Universitas Indonesia, Kampus UI Depok, West Java 16424, Indonesia
[4]Interdisciplinary Program of Bioenergy and Biomaterial Engineering, Chonnam National University, Gwangju 500-757, Republic of Korea
[5]Department of Biotechnology and Bioengineering, Chonnam National University, Gwangju 500757, Republic of Korea

Abstract. Bone damage is one of the main causes of disability in humans, and tissue engineering technology by applying biomaterial-based scaffold has been developed as an effective solution. This can be achieved using various natural and synthetic polymers combined with carbon-based and metal-oxide materials. Therefore, this study aimed to develop bone scaffold using collagen, alginate, and poly(vinyl alcohol), with the addition of multi-walled carbon nanotube, reduced graphene oxide, titanium dioxide, and zinc oxide materials. Scaffold was fabricated with the freeze-drying method and characterized physicochemically by observing the morphology through scanning electron microscopy (SEM), identification of functional groups by Fourier transform infrared spectroscopy (FTIR), compressive mechanical properties, porosity, and degradation rate. The results showed that each group of scaffold had a compact structure, with a small pore size and less than 50% porosity. The functional groups of each material were detected, and the compressive strength matched the trabecular bone, approximately 6 MPa. However, the scaffold lacked appropriate porosity and a fast degradation rate exceeding 35% in 7 days.

Keywords: Biomaterials; Bone Scaffold; Carbon materials; Metal oxide materials; Physical and chemical characterization

1. Introduction

Osteoarthritis is one of the most common public health problems, affecting approximately 10% of the global population older than 60 years (Yahaya *et al.,* 2021). The number of cases worldwide increased from 247.51 million in 1990 to 527.81 million in 2019, with prevalence rising by 113.25%. Concurrently, there has been a rapid rise in age-

standardized years living with disability due to osteoarthritis by 114.5% from 1990 to 2019 (Long *et al.,* 2022).

Tissue engineering, a multifaceted process aimed at replacing damaged organs, entails restoring various biological functions (Amiryaghoubi *et al.,* 2022). In this context, biomaterial-based scaffold has been developed to support cell adhesion, growth, and determine compatibility with the body (Zhang *et al.,* 2023). An ideal scaffold for tissue engineering applications should have optimal chemical and structural characteristics along with good mechanical properties (Jafari *et al.,* 2017). In addition, scaffold is expected to have good microstructure, such as high porosity with appropriate pore size and permeability, to support cartilage regeneration (Wasyłeczko, Sikorska, and Chwojnowski, 2020; Bružauskaitė *et al.,* 2016).

Various naturally-derived polymers have been used as bone tissue scaffold, and synthetic polymers can also be incorporated alongside natural ones to improve hydrophilicity, cell adhesion, and biodegradability (Jafari *et al.,* 2017). Collagen is a major component of the extracellular matrix (ECM) and one of the most frequently used biomaterials in protein-based scaffold for bone tissue engineering (Zhang *et al.,* 2018). Alginate is a natural polysaccharide with wider availability, good biocompatibility, and ease of gelation (Hu and Lo, 2021). The addition to the scaffold is an easy and effective way to increase porosity and suitability for use as a matrix (Chandika *et al.,* 2015). However, collagen and alginate have limitations in the mechanical stability, showing the need to add other polymers with higher mechanical capacity (Shirehjini *et al.,* 2022). Poly(vinyl alcohol) (PVA) is a synthetic polymer with good biocompatibility, biodegradability, high hydrophilicity, and mechanical resistance as a scaffold material (Rochardjo *et al.,* 2021).

Carbon-based materials are advantageous by providing electrical conductivity, mechanical reinforcement, and high surface area (Massoumi *et al.,* 2021). Previous studies showed that multi-walled carbon nanotube (MWCNT) scaffold had good characteristics for adhesion, proliferation, and osteogenesis differentiation (Xu *et al.,* 2019). Meanwhile, graphene-based materials and the derivatives, such as graphene oxide (GO) and reduced graphene oxide (rGO), which possess high surface area and electrical conductivity (Hardi and Rahman, 2020), have also been investigated to enhance cell attachment and differentiation (Sanati *et al.,* 2022).

Metal oxide nanoparticles are more widely used due to the better quality and less toxicity compared to carbon materials (Shalaby, Anwar, and Saeed, 2022). One common example is Zinc oxide (ZnO) nanoparticles with good antibacterial and biocompatibility properties (Christy Basha, and Kumari, 2022). Others, such as titanium dioxide (TiO_2), are also high-conductivity materials with chemical stability and low toxicity (Khalil *et al.,* 2019). As stated in a previous study, TiO_2 is capable of facilitating osteoblast cell adhesion while enhancing the antibacterial ability of the scaffold (Cao *et al.,* 2018). Therefore, this study aimed to develop bone scaffold using collagen (Col), alginate (Alg), and PVA, with the addition of MWCNT, rGO, TiO_2, and ZnO materials, to aid the cartilage regeneration process.

2. Methods

2.1. Materials

King cobia collagen was extracted using the deep eutectic solvent method adapted from Batista *et al.* (2022). MWCNT 95% [Sigma Aldrich] was functionalized by adapting Shrestha *et al.* (2017), and reduced graphene oxide was reduced using graphene oxide (≥ 50% of carbon) [Sigma Aldrich] based on Habte and Ayele (2019). TiO_2 was synthesized with titanium trichloride 15% [Sigma Aldrich] according to Fayyadh *et al.* (2019), and zinc oxide was prepared using zinc acetate dihydrate 99.5% [Sigma Aldrich] in line with Haque *et al.*

(2020). Sodium hydroxide 99% to neutralize pH and ethanol 99% were purchased from Merck. Meanwhile, sodium alginate powder, poly(vinyl alcohol) 98% hydrolyzed, acetic acid (glacial) 100%, and phosphate-buffered saline were all purchased from Sigma Aldrich.

2.2. Fabrication of Scaffold

The development of scaffold commenced with the preparation of collagen, sodium alginate, and PVA solutions. Collagen material was dissolved in 0.5 M acetic acid to obtain a 2 wt% solution, which was further added with 2 M NaOH to adjust the pH to neutral. Alginate material was dissolved in distilled water with stirring at 40°C for 2 hours to obtain 1 wt% solution. Meanwhile, PVA material was dissolved in distilled water with stirring at 80°C for 2 hours to obtain a 5 wt% solution. The collagen solution was mixed with the alginate and stirred for 2 hours to produce a homogeneous solution. Subsequently, PVA solution was mixed with Col/Alg mixture and stirred for 2 hours.

Each Col/Alg/PVA container was added with 0.5 wt% MWCNT, 0.1 wt% rGO, 1 wt% ZnO, and 1 wt% TiO_2 separately according to the container. Stirring was carried out for 2 hours with sonication for 1 hour. Each container was then transferred to a 48-well tissue culture plate. The four scaffold groups were frozen in a freezer at -80°C for 24 hours and freeze-dried for 48 hours.

2.3. Scaffold Characterization

2.3.1. Scanning Electron Microscopy (SEM) Characterization

The morphology of the scaffold was observed through SEM (Zeiss, EVO-MA10) with an acceleration voltage of 15 kV. Specimens were coated before observing scaffold surface.

2.3.2. Fourier Transform Infrared Spectroscopy (FTIR) Characterization

The functional groups in the sample material were characterized using FTIR (Thermo Scientific Nicolet iS10).

2.3.3. Mechanical Compressive Test

A compressive test was conducted to determine the durability parameters of the scaffold. This was conducted through Instron's Universal Testing Machine (UTM) using the ASTM D143 standard with a compressive force rate of 10 mm/minute until it reached a change in the shape of the scaffolding to be destroyed. Scaffold used for the compressive test had a diameter of 10 mm and a height of 5 mm in each group. It was then placed in a horizontal position in the middle between the pressure plate and the compressive force was applied in a downward pressure direction to determine the strength limit of scaffold.

2.3.4. Porosity

The porosity test, aimed at observing the porosity of scaffold surface, was conducted by the liquid displacement method. Scaffold was cut into pieces, with the volume determined first by measuring the diameter (D) and height (H). The dry sample was weighed (Wd) and immersed in 10 mL ethanol at room temperature for 5 minutes. Filtration was conducted with filter paper to remove excess ethanol, then the wet weight (Wp) was immediately weighed. The porosity was calculated using Equation (1), where ρ is the density of ethanol (ρ = 0.789 g/cm³) (Jing *et al.*, 2017).

$$Porosity\ (\%) = \frac{w_p - w_d}{\rho \pi \left(\frac{D}{2}\right)^2 H} \times 100 \tag{1}$$

2.3.5. Degradation Rate

The degradation test was conducted to determine scaffold ability when dissolved in the body. The test was conducted by dissolving the weighed dry scaffold in 10 mL PBS (pH 7.4), which was designed to mimic the body environment when cells would be grown, with intervals of H+1, H+5, and H+7. The dissolved product was incubated at 37°C and filtered

using filter paper to remove excess PBS. Scaffold was oven-dried at 70°C for 40 minutes until the water content disappeared, and the final weight (Wt) was weighed. The percentage degradation rate was calculated using Equation (2) (Gholizadeh *et al.*, 2017).

$$\text{Degradation rate (\%)} = \frac{w_d - w_t}{w_d} \times 100$$

(2)

2.4. Statistical and Graphical Analysis

Statistical analysis was performed to compare test values for each physicochemical characteristic. All quantitative experimental data were represented as mean ± standard deviation with 3 repetitions for each test.

3. Results and Discussion

3.1. Scaffold Characterization

3.1.1. SEM Characterization

SEM characterization was performed on each group of Col/Alg/PVA scaffold with the addition of MWCNT, rGO, TiO$_2$, and ZnO to determine and compare the morphology as well as topography. This was conducted to provide valuable information regarding the potential for cell interactions with scaffold structure.

Figure 1(a) shows SEM image morphology of Col/Alg/PVA/MWCNT scaffold to have a rough surface with fairly wide gaps (marked with red arrows). Thickening of the pore walls could reduce porosity, lowering the area available for cell growth. As shown in Figure 1(b), SEM image morphology of Col/Alg/PVA/rGO scaffold had a dense and interconnected structure but possessed tiny pores. This was in accordance with Kavya *et al.* (2013), stating that the high density caused a reduction in porosity but contributed to high mechanical strength (Kavya *et al.*, 2013). Figure 1(c) shows that SEM image morphology of Col/Alg/PVA/TiO$_2$ scaffold has a rough but interconnected structure. There were fibers from collagen fused with other materials, including TiO$_2$ particles (marked with red arrows). Figure 1(d) shows SEM image morphology of Col/Alg/PVA/ZnO scaffold to have a dense but interconnected structure. Scaffold also had fairly wide gaps (marked with red arrows) but did not show interconnected pores.
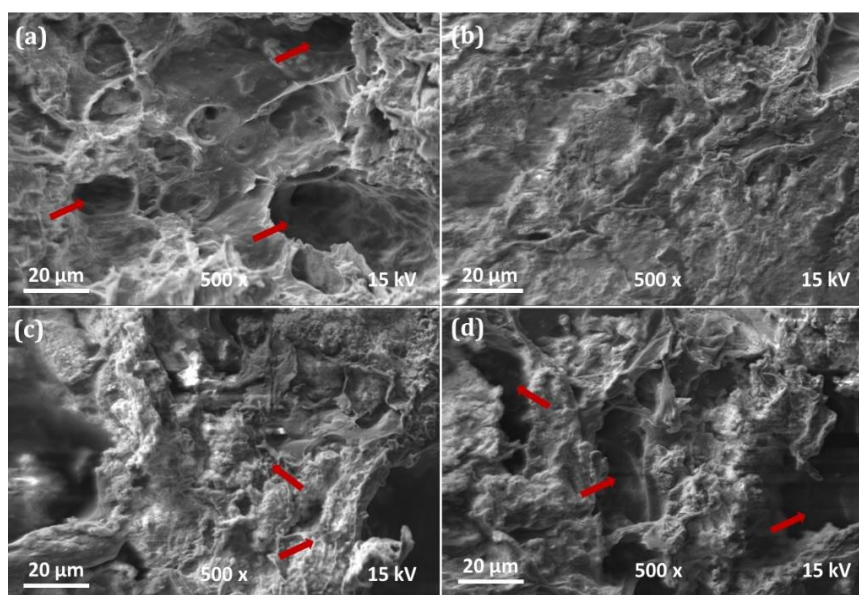

Figure 1 SEM results of Col/Alg/PVA scaffold with the addition of (a) MWCNT, (b) rGO, (c) TiO$_2$, and (d) ZnO

Based on SEM characterization results, the pore sizes of the four scaffold groups did not meet the required minimum pore size. Although the pore size was generally small, it could indirectly benefit cell growth, by increasing their retention. This was proven in the study by Kosowska *et al.* (2020), showing that smaller pores could increase cell proliferation and cellular interactions. According to Morejón *et al.* (2019), a micropore size of approximately <10 μm created a larger surface area that stimulated greater ion exchange and bone protein adsorption.

3.1.2. FTIR Characterization of Scaffold

FTIR characterization was performed on each group of Col/Alg/PVA scaffold with the addition of MWCNT, rGO, TiO$_2$, and ZnO to determine the content of functional groups resulting from the mixture of materials. The collagen absorption peaks comprised 3306 cm^{-1} (N-H group stretching vibrations), 1632 cm^{-1} (amide I bond), 1546 cm^{-1} (amide II bond), and 1236 cm^{-1} (amide III bond). Sodium alginate peaks included 3402 cm^{-1} (hydroxyl (O-H) bonds), 2926 cm^{-1} (CH$_2$ groups), 1607 cm^{-1} and 1410 cm^{-1} (asymmetric and symmetric –COO stretches), 1607 cm^{-1} (C=O carboxyl bonds), and 1031 cm^{-1} (antisymmetric C-O-C stretches) (Sobhanian *et al.*, 2019). Meanwhile, the peak spectrum of PVA showed a broad absorption band at 3000–3600 cm^{-1} attributed to hydroxyl group symmetrical stretching, and 1090 cm^{-1} representing the carboxyl vibration (–CO–) of PVA (Cao *et al.*, 2018).

Figure 2 shows FTIR results on all scaffold groups with each having carboxyl, hydroxyl, and amide groups. The presence of hydroxyl (–OH) and carboxyl (–COOH) groups enhanced the formation of many hydrogen bonds with water molecules (Dibazar *et al.*, 2022). Furthermore, the acquisition of amide groups on scaffold played a significant role in organic chemical activity and cell biology associated with the structure of proteins, enzymes, polypeptides, and other biological molecules (Jia *et al.*, 2013).
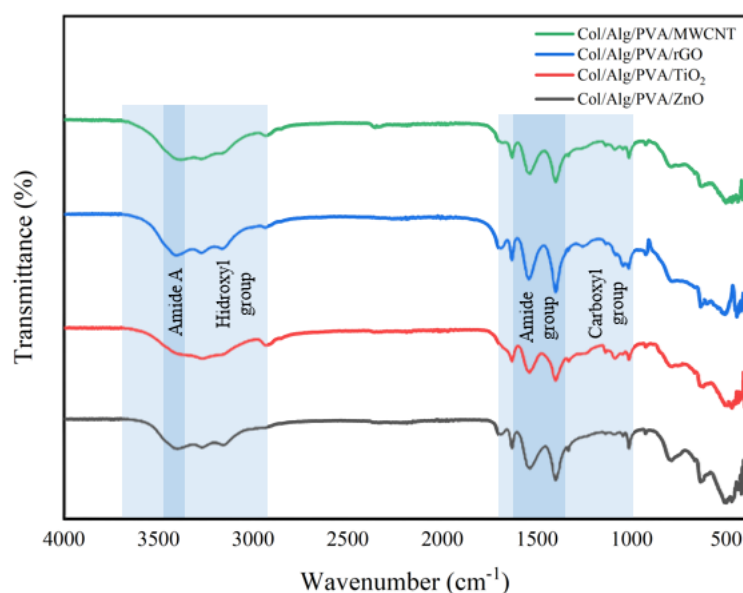

Figure 2 FTIR graph of Col/Alg/PVA scaffold with added MWCNT, rGO, TiO$_2$, and ZnO materials

3.1.3. Mechanical Compressive Test of Scaffold

Mechanical testing of scaffold was conducted to determine the compressive strength and compare with the mechanical characteristics of bone, as shown in Figure 3.
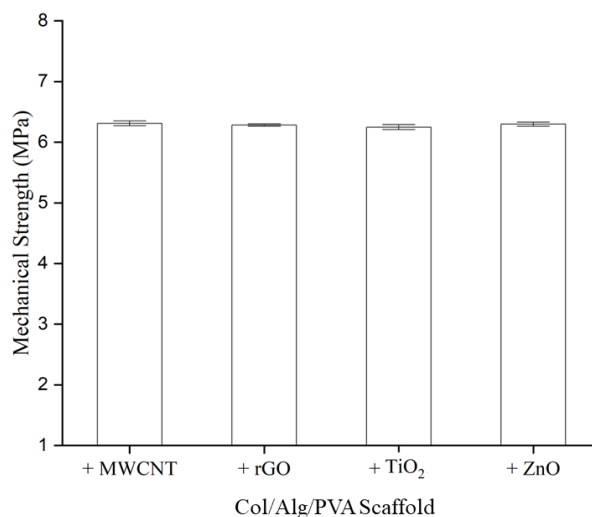
Figure 3 Mean and standard deviation of compressive test results of Col/Alg/PVA scaffold with the addition of MWCNT, rGO, TiO₂, and ZnO materials

One of the characteristics of an ideal scaffold for tissue engineering is having a mechanical strength similar to native bone tissue. The compressive strength for each scaffold group was about 6 MPa, meeting the mechanical criteria for trabecular bone (0,1–16 MPa) but not for cortical bone (130–200 MPa) (Gerhardt and Boccaccini, 2010). The mechanical properties tended to decrease exponentially with increasing porosity (Abbasi *et al.*, 2020). The compressive test results were relatively large with small porosity. This implied that the addition of MWCNT, rGO, TiO₂, and ZnO materials did not affect mechanical strength of Col/Alg/PVA scaffold.

3.1.4. Scaffold Porosity

The porosity test was conducted to determine the nature of scaffold to support cell proliferation and migration. The results in Figure 4 showed that the addition of MWCNT, rGO, TiO₂, and ZnO materials did not significantly affect the porosity of Col/Alg/PVA scaffold. The porosity of the four scaffold groups was relatively small and fell below the desired specifications. Porosity results with a 50–90% percentage range are considered optimal (Mishra *et al.*, 2019). However, several studies found an important role of low porosity. In Liu *et al.* (2018), it was found that lower pore size was associated with the formation of osteoid or fibrous tissue.
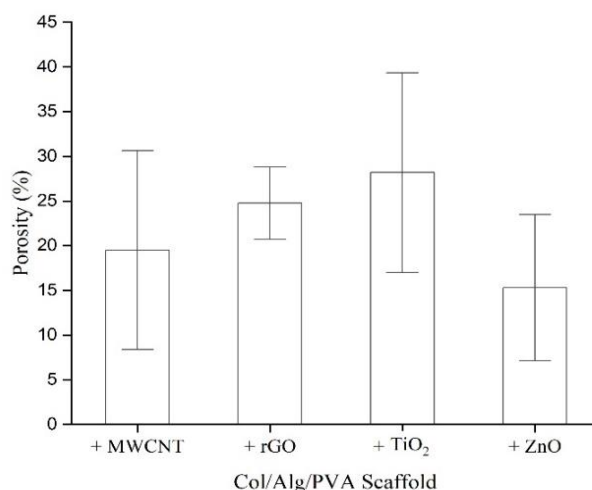

Figure 4 Mean and standard deviation of porosity test results of Col/Alg/PVA scaffold with added MWCNT, rGO, TiO₂, and ZnO materials

3.1.5. Scaffold Degradation Rate

The degradation rate of good scaffold for tissue engineering should match the rate of new tissue formation to meet the necessary conditions (Alizadeh *et al.*, 2013). The results (Figure 5) showed a fairly stable weight loss as the duration of the test increased. Scaffold with a favorable degradation rate should be compatible with the maturation and regeneration time of new tissue after in vivo transplantation (Wissing *et al.*, 2017). Several factors, including pore homogeneity, morphology, and pore size, can cause high degradation rates. Furthermore, scaffold with better mechanical properties also have slower degradation rates (Diogo *et al.*, 2018). Based on the results, the addition of rGO material reduced the degradation rate with fairly good strength. All four groups had a high degradation rate for 7 days, showing that the scaffold did not meet the desired specifications in the degradation test parameters.
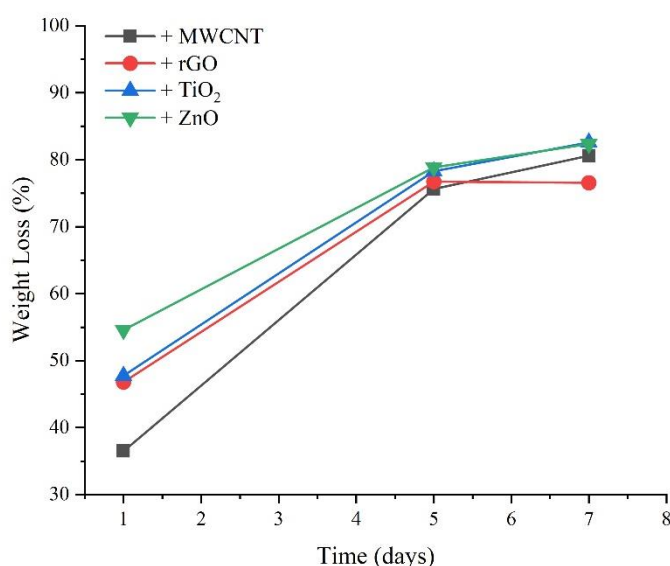

Figure 5 Mean and standard deviation of degradation rate test results of Col/Alg/PVA scaffold with the addition of MWCNT, rGO, TiO2, and ZnO materials

4. Conclusions

In conclusion, SEM results showed that scaffold had a dense and bonded structure but lacked the appropriate pore size and porosity. All four groups had a high swelling percentage with a high degradation rate. There was no significant difference between each group in terms of mechanical characterization and porosity test. This implied that the addition of MWCNT, rGO, TiO2, and ZnO materials did not affect the physicochemical characteristics of Col/Alg/PVA scaffold. Therefore, fabricated scaffold cannot be used as a candidate for bone tissue engineering, and further development is needed regarding the composition and concentration of the materials added.

Acknowledgments

References

Abbasi, N., Hamlet, S., Love, R.M., Nguyen, N.-T., 2020. Porous Scaffolds for Bone Regeneration. *Journal of Science: Advanced Materials and Devices,* Volume 5, pp. 1–9

Alizadeh, M., Abbasi, F., Khoshfetrat, A.B., Ghaleh, H., 2013. Microstructure and Characteristic Properties of Gelatin/Chitosan Scaffold Prepared by A Combined Freeze-Drying/Leaching Method. *Materials Science and Engineering C,* Volume 33, pp. 3958–3967

Amiryaghoubi, N., Fathi, M., Barar, J., Omidi, Y., 2022. Hydrogel-Based Scaffolds for Bone and Cartilage Tissue Engineering and Regeneration. *Reactive and Functional Polymers,* Volume 177, p. 105313

Batista, M.P., Fernández, N., Gaspar, F.B., Bronze, M. do R., Duarte, A.R.C., 2022. Extraction of Biocompatible Collagen from Blue Shark Skins Through the Conventional Extraction Process Intensification Using Natural Deep Eutectic Solvents. *Frontiers in Chemistry,* Volume 10, p. 937036

Bružauskaitė, I., Bironaitė, D., Bagdonas, E., Bernotienė, E., 2016. Scaffolds and Cells for Tissue Regeneration: Different Scaffold Pore Sizes—Different Cell Effects. *Cytotechnology,* Volume 68, pp. 355–369

Cao, L., Wu, X., Wang, Q., Wang, J., 2018. Biocompatible Nanocomposite of TiO2 Incorporated Bi-Polymer for Articular Cartilage Tissue Regeneration: A Facile Material. *Journal of Photochemistry and Photobiology B: Biology,* Volume 178, pp. 440–446

Chandika, P., Ko, S.-C., Oh, G.-W., Heo, S.-Y., Nguyen, V.-T., Jeon, Y.-J., Lee, B., Jang, C.H., Kim, G., Park, W.S., Chang, W., Choi, I.-W., Jung, W.-K., 2015. Fish Collagen/Alginate/Chitooligosaccharides Integrated Scaffold for Skin Tissue Regeneration Application. *International Journal of Biological Macromolecules,* Volume 81, pp. 504–513

Christy, P.N., Basha, S.K., Kumari, V.S., 2022. Nano Zinc Oxide And Nano Bioactive Glass Reinforced Chitosan/Poly(Vinyl Alcohol) Scaffolds For Bone Tissue Engineering Application. *Materials Today Communications,* Volume 31, p. 103429

Dibazar, Z.E., Mohammadpour, M., Samadian, H., Zare, S., Azizi, M., Hamidi, M., Elboutachfaiti, R., Petit, E., Delattre, C., 2022. Bacterial Polyglucuronic Acid/Alginate/Carbon Nanofibers Hydrogel Nanocomposite as a Potential Scaffold for Bone Tissue Engineering. *Materials*, Volume 15, p. 2494

Diogo, G., López-Senra, E., Pirraco, R., Canadas, R., Fernandes, E., Serra, J., Pérez-Martín, R., Sotelo, C., Marques, A., González, P., Moreira-Silva, J., Silva, T., Reis, R., 2018. Marine Collagen/Apatite Composite Scaffolds Envisaging Hard Tissue Applications. *Marine Drugs,* Volume 16, p. 269

Fayyadh, A.A., Essa, A.F., Batros, S.S., Shallal, Z.S., 2019. Studying the Crystal Structure, Topography, and Antibacterial of a Novel Titania (TiO$_2$ NPs) Prepared by a Sol-gel Manner. *Baghdad Science Journal,* Volume 16, p. 0910

Gerhardt, L.C., Boccaccini, A.R., 2010. Bioactive Glass and Glass-Ceramic Scaffolds for Bone Tissue Engineering. *Materials,* Volume 3, pp. 3867–3910

Gholizadeh, S., Moztarzadeh, F., Haghighipour, N., Ghazizadeh, L., Baghbani, F., Shokrgozar, M.A., Allahyari, Z., 2017. Preparation And Characterization of Novel Functionalized Multi-Walled Carbon Nanotubes/Chitosan/B-Glycerophosphate Scaffolds for Bone Tissue Engineering. *International Journal of Biological Macromolecules,* Volume 97, pp. 365–372

Habte, A.T., Ayele, D.W., 2019. Synthesis and Characterization of Reduced Graphene Oxide (rGO) Started from Graphene Oxide (GO) Using the Tour Method with Different Parameters. *Advances in Materials Science and Engineering,* Volume 2019, pp. 1–9

Haque, M.J., Bellah, M.M., Hassan, M.R., Rahman, S., 2020. Synthesis of ZnO Nanoparticles by Two Different Methods & Comparison of Their Structural, Antibacterial, Photocatalytic and Optical Properties. *Nano Express,* Volume 1(1), p. 010007

Hardi, G.W., Rahman, S.F., 2020. Amperometric Detection of Dopamine based on a Graphene Oxide/PEDOT:PSS Composite Electrode. *International Journal of Technology,* Volume 11(5), pp. 974–983

Hu, T., Lo, A.C.Y., 2021. Collagen–Alginate Composite Hydrogel: Application in Tissue Engineering and Biomedical Sciences. *Polymers (Basel),* Volume 13, p. 1852

Jafari, M., Paknejad, Z., Rad, M.R., Motamedian, S.R., Eghbal, M.J., Nadjmi, N., Khojasteh, A., 2017. Polymeric Scaffolds in Tissue Engineering: A Literature Review. *Journal of Biomedical Materials Research Part B: Applied Biomaterials,* Volume105, pp. 431–459

Jia, L., Duan, Z., Fan, D., Mi, Y., Hui, J., Chang, L., 2013. Human-Like Collagen/Nano-Hydroxyapatite Scaffolds for The Culture of Chondrocytes. *Materials Science and Engineering C*, Volume 33(2), pp. 727–734

Jing, Z., Wu, Y., Su, W., Tian, M., Jiang, W., Cao, L., Zhao, L., Zhao, Z., 2017. Carbon Nanotube Reinforced Collagen/Hydroxyapatite Scaffolds Improve Bone Tissue Formation In Vitro and In Vivo. *Annals of Biomedical Engineering*, Volume 45, pp. 2075–2087

Kavya, K.C., Jayakumar, R., Nair, S., Chennazhi, K.P., 2013. Fabrication And Characterization of Chitosan/Gelatin/nSiO2 Composite Scaffold for Bone Tissue Engineering. *International Journal of Biological Macromolecules,* Volume 59, pp. 255–263

Khalil, M., Rahmaningsih, G., Gunlazuardi, J., Umar, A., 2019. The Influence of Plasmonic Au Nanoparticle Integration on the Optical Bandgap of Anatase TiO_2 Nanoparticles. *International Journal of Technology,* Volume 10(4), pp. 808–817

Kosowska, K., Domalik-Pyzik, P., Sekuła-Stryjewska, M., Noga, S., Jagiełło, J., Baran, M., Lipińska, L., Zuba-Surma, E., Chłopek, J., 2020. Gradient Chitosan Hydrogels Modified with Graphene Derivatives and Hydroxyapatite: Physiochemical Properties and Initial Cytocompatibility Evaluation. *International Journal of Molecular Sciences,* Volume 21, p. 4888

Liu, J., Chen, G., Xu, H., Hu, K., Sun, J., Liu, M., Zhang, F., Gu, N., 2018. Pre-Vascularization in Fibrin Gel/PLGA Microsphere Scaffolds Designed for Bone Regeneration. *NPG Asia Materials,* Volume 10, pp. 827–839

Long, H., Liu, Q., Yin, H., Wang, K., Diao, N., Zhang, Y., Lin, J., Guo, A., 2022. Prevalence Trends of Site-Specific Osteoarthritis From 1990 to 2019: Findings from the Global Burden of Disease Study 2019. *Arthritis & Rheumatology,* Volume 74, pp. 1172–1183

Massoumi, B., Abbasian, M., Khalilzadeh, B., Jahanban-Esfahlan, R., Rezaei, A., Samadian, H., Derakhshankhah, H., Jaymand, M., 2021. Gelatin-Based Nanofibrous Electrically Conductive Scaffolds for Tissue Engineering Applications. *International Journal of Polymeric Materials and Polymeric* Biomaterials, Volume 70, pp. 693–702

Mishra, R., Varshney, R., Das, N., Sircar, D., Roy, P., 2019. Synthesis and characterization of gelatin-PVP polymer composite scaffold for potential application in bone tissue engineering. Eur Polym J 119, 155–168

Morejón, L., Delgado, J.A., Antunes Ribeiro, A., Varella de Oliveira, M., Mendizábal, E., García, I., Alfonso, A., Poh, P., van Griensven, M., Balmayor, E.R., 2019. Development, Characterization and In Vitro Biological Properties of Scaffolds Fabricated from Calcium Phosphate Nanoparticles. *International Journal of Molecular Sciences,* Volume 20, p. 1790

Rochardjo, H.S., Fatkhurrohman, F., Kusumaatmaja, A., Yudhanto, F., 2021. Fabrication of Nanofiltration Membrane based on Polyvinyl Alcohol Nanofibers Reinforced with

Cellulose Nanocrystal using Electrospinning Techniques. *International Journal of Technology,* Volume 12(2), pp. 329–338

Sanati, A., Kefayat, A., Rafienia, M., Raeissi, K., Siavash Moakhar, R., Salamat, M.R., Sheibani, S., Presley, J.F., Vali, H., 2022. A Novel Flexible, Conductive, and Three-Dimensional Reduced Graphene Oxide/Polyurethane Scaffold for Cell Attachment and Bone Regeneration. *Materials & Design,* Volume 221, p. 110955

Shalaby, M.A., Anwar, M.M., Saeed, H., 2022. Nanomaterials for Application in Wound Healing: Current State-Of-The-Art and Future Perspectives. *Journal of Polymer Research*, Volume 29(3), p. 91

Shirehjini, L.M., Sharifi, F., Shojaei, S., Irani, S., 2022. Poly-Caprolactone Nanofibrous Coated with Sol-Gel Alginate/ Mesenchymal Stem Cells for Cartilage Tissue Engineering. *Journal of Drug Delivery Science and Technology,* Volume 74, p. 103488

Shrestha, B.K., Shrestha, S., Tiwari, A.P., Kim, J.-I., Ko, S.W., Kim, H.-J., Park, C.H., Kim, C.S., 2017. Bio-Inspired Hybrid Scaffold of Zinc Oxide-Functionalized Multi-Wall Carbon Nanotubes Reinforced Polyurethane Nanofibers for Bone Tissue Engineering. *Materials & Design,* Volume 133, pp. 69–81

Sobhanian, P., Khorram, M., Hashemi, S.-S., Mohammadi, A., 2019. Development of Nanofibrous Collagen-Grafted Poly (Vinyl Alcohol)/Gelatin/Alginate Scaffolds as Potential Skin Substitute. *International Journal of Biological Macromolecules,* Volume 130, pp. 977–987

Wasyłeczko, M., Sikorska, W., Chwojnowski, A., 2020. Review of Synthetic and Hybrid Scaffolds in Cartilage Tissue Engineering. *Membranes (Basel),* Volume 10, p. 348

Wissing, T.B., Bonito, V., Bouten, C.V.C., Smits, A.I.P.M., 2017. Biomaterial-Driven in Situ Cardiovascular Tissue Engineering—A Multi-Disciplinary Perspective. *NPJ Regenerative Medicine,* Volume 2, p. 18

Xu, J., Hu, X., Jiang, S., Wang, Y., Parungao, R., Zheng, S., Nie, Y., Liu, T., Song, K., 2019. The Application of Multi-walled Carbon Nanotubes in Bone Tissue Repair Hybrid Scaffolds and the Effect on Cell Growth In Vitro. *Polymers (Basel),* Volume 11, p. 230

Yahaya, I., Wright, T., Babatunde, O.O., Corp, N., Helliwell, T., Dikomitis, L., Mallen, C.D., 2021. Prevalence of Osteoarthritis in Lower Middle- and Low-Income Countries: A Systematic Review and Meta-Analysis. *Rheumatology International,* Volume 41, pp. 1221–1231

Zhang, D., Wu, X., Chen, J., Lin, K., 2018. The Development of Collagen Based Composite Scaffolds for Bone Regeneration. *Bioactive Materials,* Volume 3, pp. 129–138.

Zhang, W., Hou, X., Wang, H., Kong, D., Zhou, Y., 2023. Preparation of Chitosan-Sodium Alginate/Bioactive Glass Composite Cartilage Scaffolds with High Cell Activity and Bioactivity. *Ceramics International,* Volume 49(2), pp. 1987–1996